

Structure Functions - Status and Prospect

J. C. Peng

University of Illinois, Urbana, Illinois, 61801, U.S.A.

Abstract. Current status and future prospects of the structure functions and parton distribution studies are presented.

INTRODUCTION

The study of nucleon's structure functions and parton distributions is an active area of research in nuclear and particle physics. The parton distributions address both the perturbative and nonperturbative aspects of QCD, and they also provide an essential input for describing hard processes in high-energy hadron collisions. As a result of several decades's intense effort, the unpolarized proton structure functions have been well mapped out over a broad range of Q^2 and Bjorken- x . While these data are invaluable for testing QCD and for extracting various parton distributions, several questions remain unanswered. For example, the unexpected finding of the flavor asymmetry of the light-quark sea (\bar{u}, \bar{d}) suggests that other aspects of the flavor structure, such as possible asymmetry between the s and \bar{s} sea quark distributions and the behavior of valence d/u ratio at large x , need to be examined. The issue of quark-hadron duality, as reflected in the intriguing similarity between the structure functions measured at the resonance region and at the DIS region, also requires further studies.

Remarkable progress in the study of spin-dependent structure functions has been made since the discovery of the "proton spin puzzle" in the late 1980's. Very active spin-physics programs have been pursued at many facilities including SLAC, CERN, HERA, JLab, and RHIC. The polarized DIS data now cover a sufficiently broad Q^2 range for scaling-violation to be observed. In recent years, new experimental tools such as semi-inclusive polarized DIS, polarized proton-proton collision, and deeply exclusive reactions have been employed to address the major unresolved question in spin physics: How is the proton's spin distributed among its various constituents?

On the theory front, the formulation of the generalized parton distributions as well as the identification of various k_T (intrinsic transverse momentum of partons)-dependent structure and fragmentation functions have opened exciting new directions of research. Furthermore, important progress in the Lattice calculations for the moments of various parton distributions and in the extrapolations to their chiral limits has been made.

In this review I will focus on recent progress in the following areas:

- Flavor structure of parton distributions
- Transition from high- Q^2 to low- Q^2
- Novel distribution and fragmentation functions; Generalized parton distributions

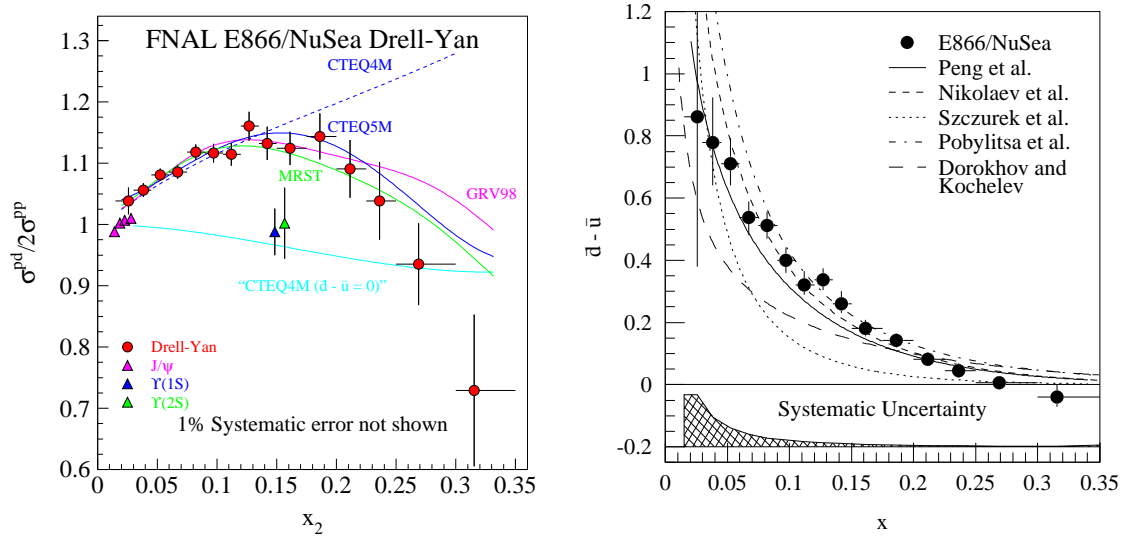


FIGURE 1. Left panel: Cross section ratios of $p+d$ over $2(p+p)$ for Drell-Yan, J/Ψ , and Υ production from FNAL E866. Right panel: Comparison of E866 $\bar{d} - \bar{u}$ data with calculations from various models [2].

FLAVOR STRUCTURES OF PARTON DISTRIBUTIONS

\bar{d}/\bar{u} flavor asymmetry

The earliest parton models assumed that the proton sea was flavor symmetric, even though the valence quark distributions are clearly flavor asymmetric. The flavor symmetry assumption was not based on any known physics, and it remained to be tested. Under the assumption of a \bar{u} , \bar{d} flavor-symmetric sea in the nucleon, the Gottfried Sum Rule [1], $I_G = \int_0^1 (F_2^p(x, Q^2) - F_2^n(x, Q^2))/x dx = 1/3$, is obtained. The NMC collaboration determined the Gottfried integral to be 0.235 ± 0.026 , significantly below $1/3$. This surprising result can be explained by a large flavor asymmetry between the \bar{u} and the \bar{d} .

The x dependence of \bar{d}/\bar{u} asymmetry has been determined by proton-induced Drell-Yan (DY) as well as semi-inclusive DIS measurements. Figure 1 shows that the Fermilab E866 [2] DY cross section per nucleon for $p+d$ clearly exceeds $p+p$, and it indicates an excess of \bar{d} with respect to \bar{u} over an appreciable range in x . In contrast, the $\sigma(p+d)/2\sigma(p+p)$ ratios for J/Ψ and Υ production, also shown in Fig. 1, are very close to unity. This reflects the dominance of gluon-gluon fusion process for quarkonium production and the expectation that the gluon distributions in the proton and in the neutron are identical.

Many theoretical models, including meson cloud model, chiral-quark model, Pauli-blocking model, instanton model, chiral-quark soliton model, and statistical model, have been proposed to explain the \bar{d}/\bar{u} asymmetry. For recent reviews, see [3, 4]. These models can describe the $\bar{d} - \bar{u}$ data very well, as shown in Fig. 1. However, they all have difficulties explaining the \bar{d}/\bar{u} data at large x ($x > 0.2$). The new 120 GeV Fermilab Main Injector and the proposed 50 GeV Japanese Hadron Facility present opportunities for extending the \bar{d}/\bar{u} measurement to larger x ($0.25 < x < 0.7$).

Models in which virtual mesons are admitted as degrees of freedom have implications that extend beyond the \bar{d}, \bar{u} flavor asymmetry addressed above. They create hidden strangeness in the nucleon via such virtual processes as $p \rightarrow \Lambda + K^+, \Sigma + K$, etc. Such processes are of considerable interest as they imply different s and \bar{s} parton distributions in the nucleon, a feature not found in gluonic production of $s\bar{s}$ pairs.

A difference between the s and \bar{s} distribution can be made manifest by direct measurements of the s and \bar{s} parton distribution functions in neutrino DIS. A fit to the CDHS neutrino charged-current inclusive data together with charged lepton DIS data found evidence for $\int_0^1 s(x)dx > \int_0^1 \bar{s}(x)dx$ [5]. However, an analysis [6] of the recent CCFR and NuTeV $\nu(\bar{\nu})N \rightarrow \mu^+\mu^-x$ dimuon production data [7] favored $\int_0^1 s(x)dx < \int_0^1 \bar{s}(x)dx$ ($\int_0^1 (s(x) - \bar{s}(x))dx = -0.0027 \pm 0.0013$). To better determine the s/\bar{s} asymmetry, an NLO analysis is currently underway [8]. Violation of the s/\bar{s} symmetry would have impact on the recent extraction [9] of $\sin^2\theta_W$ from the CCFR/NuTeV νN scattering data.

Asymmetry in the s, \bar{s} distributions can also be revealed in the measurements of the strange quark's contribution to the nucleon's electromagnetic and axial form factors. These “strange” form factors can be measured in neutrino elastic scattering [10] from the nucleon, or by selecting the parity-violating component of electron-nucleon elastic scattering. Two completed parity-violating experiments [11, 12] suggest small contributions of strange quarks to nucleon form factors. Several new experiments are underway at JLab and MAMI to measure parity-violating asymmetry at various kinematic regions.

Flavor structure of polarized nucleon sea

The flavor structure and the spin structure of the nucleon sea are closely connected. Many theoretical models originally proposed to explain the \bar{d}/\bar{u} flavor asymmetry also have specific implications for the spin structure of the nucleon sea. In the meson-cloud model, for example, a quark would undergo a spin flip upon an emission of a pseudoscalar meson ($u^\uparrow \rightarrow \pi^0(u\bar{u}, d\bar{d}) + u^\downarrow$, $u^\uparrow \rightarrow \pi^+(u\bar{d}) + d^\downarrow$, $u^\uparrow \rightarrow K^+ + s^\downarrow$, etc.). The antiquarks ($\bar{u}, \bar{d}, \bar{s}$) are unpolarized ($\Delta\bar{u} = \Delta\bar{d} = \Delta\bar{s} = 0$) since they reside in spin-0 mesons. The strange quarks (s), on the other hand, would have a negative polarization.

In the chiral-quark soliton model [13, 14], the polarized isovector distributions $\Delta\bar{u}(x) - \Delta\bar{d}(x)$ appears in leading-order (N_c^2) in a $1/N_c$ expansion, while the unpolarized isovector distributions $\bar{u}(x) - \bar{d}(x)$ appear in next-to-leading order (N_c). Therefore, this model predicts a large flavor asymmetry for the polarized sea $[\Delta\bar{u}(x) - \Delta\bar{d}(x)] > [\bar{d}(x) - \bar{u}(x)]$.

The HERMES collaboration has recently reported the extraction of $\Delta\bar{u}(x)$, $\Delta\bar{d}(x)$, and $\Delta\bar{s}(x)(= \Delta s(x))$ using polarized semi-inclusive DIS (SIDIS) data [15]. Although the statistics are still limited, the HERMES results for $\Delta\bar{u}, \Delta\bar{d}, \Delta\bar{u} - \Delta\bar{d}$, as shown in Fig. 2, are all consistent with being zero. In particular, there is no evidence for a large positive $\Delta\bar{u}(x) - \Delta\bar{d}(x)$ asymmetry as was predicted [16] by the chiral quark soliton model. Figure 2 also shows that Δs tends to be positive, in contrast to the predictions of a negative polarization of the strange sea in the analysis of inclusive DIS and hyperon decay data assuming SU(3) symmetry. However, the HERMES result of $\Delta s = 0.03 \pm 0.03 \pm 0.01$ over $0.023 < x < 0.3$ is not in disagreement with the inclusive

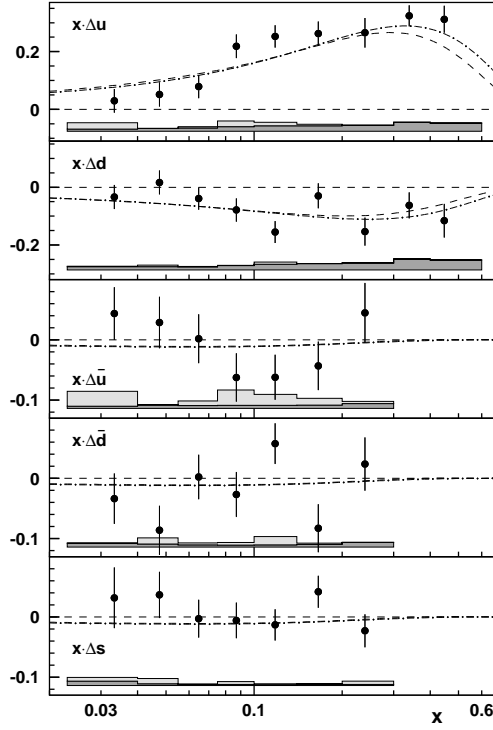


FIGURE 2. Quark and antiquark polarizations extracted from the HERMES SIDIS data [15].

DIS result of $(\Delta s + \Delta \bar{s})/2 \simeq -0.02$ [17].

Another promising technique for measuring sea-quark polarization is W -boson production [18] at RHIC. The longitudinal single-spin asymmetry for W production in polarized $p + p \rightarrow W^\pm + x$ gives a direct measure of sea-quark polarization. The RHIC W -production and the HERMES SIDIS measurements are clearly complementary tools for determining polarized sea quark distributions.

d/u ratio at large x

Another quantity related to the flavor symmetry of the proton is the d/u ratio at large x . Assuming $SU(2)_{spin} \times SU(2)_{flavor}$ symmetry, the proton wave function is given as

$$\begin{aligned}
 |p > \uparrow &= \frac{1}{\sqrt{2}} u \uparrow (ud)_{S=0, S_Z=0} + \frac{1}{\sqrt{18}} u \uparrow (ud)_{S=1, S_Z=0} - \frac{1}{3} u \downarrow (ud)_{S=1, S_Z=1} \\
 &\quad - \frac{1}{3} d \uparrow (uu)_{S=1, S_Z=0} + \frac{\sqrt{2}}{3} d \downarrow (uu)_{S=1, S_Z=1}
 \end{aligned} \tag{1}$$

The neutron wave function is readily obtained from $u \leftrightarrow d$ interchange. In nature, the $SU(2)_{spin} \times SU(2)_{flavor}$ symmetry is clearly broken, as evidenced by the large $N - \Delta$ mass splitting. The dynamic origins of this symmetry breaking remains unclear. Close and Carlitz [19, 20] argued that the dominance of the $S = 0$ diquark configuration over

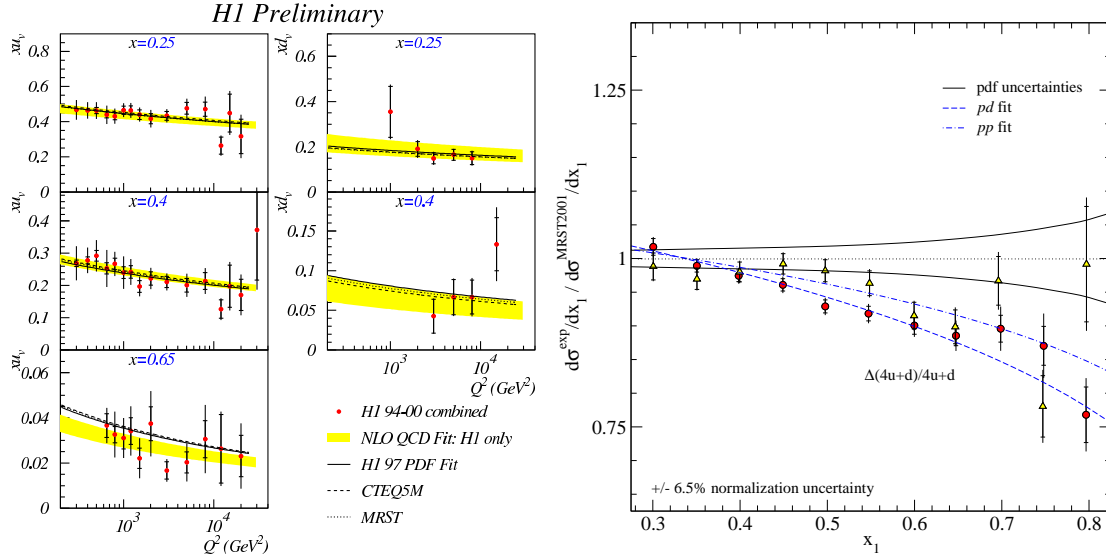


FIGURE 3. Left panel: u and d valence quark densities obtained from H1 charged-current measurements [25]. Right panel: Comparison of the E866 pp and pd DY cross sections with PDF calculations [26].

the $S = 1$ configuration would account for the $N - \Delta$ mass splitting as well as the $SU(2) \times SU(2)$ symmetry breaking. An alternative suggestion, based on perturbative QCD, was offered by Farrar and Jackson [21]. They pointed out that the spin-aligned diquark configuration with $S_Z = 1$ is suppressed since only longitudinal gluons can be exchanged. A similar result was also obtained by Brodsky et al. [22] using counting rule argument. It is straightforward to show that in the $x \rightarrow 1$ limit, the different models predict the following values for various ratios:

- $SU(2)_{\text{spin}} \times SU(2)_{\text{flavor}}$ symmetry: $\frac{d}{u} = \frac{1}{2}$, $\frac{\Delta u}{u} = \frac{2}{3}$, $\frac{\Delta d}{d} = -\frac{1}{3}$, $\frac{F_2^n}{F_2^p} = \frac{2}{3}$.
- $S = 0$ diquark dominance: $\frac{d}{u} = 0$, $\frac{\Delta u}{u} = 1$, $\frac{\Delta d}{d} = -\frac{1}{3}$, $\frac{F_2^n}{F_2^p} = \frac{1}{4}$.
- $S_Z = 0$ diquark dominance: $\frac{d}{u} = \frac{1}{5}$, $\frac{\Delta u}{u} = 1$, $\frac{\Delta d}{d} = 1$, $\frac{F_2^n}{F_2^p} = \frac{3}{7}$.

The distinct predictions for F_2^n/F_2^p from various models could be tested against DIS experiments. However, there exist considerable uncertainties in the extraction of F_2^n from the measurement of F_2^d . Depending on the treatment of the nuclear effects in the deuteron, very different values for F_2^n/F_2^p (and d/u) were obtained at large x [23]. It is clearly desirable to measure d/u without the need to model nuclear effects in the deuteron. One method is to measure the charge asymmetry of W production in $p - \bar{p}$ collision. Indeed, the CDF data [24] on the W charge asymmetry have already provided useful constraints on the d/u ratio.

The d/u ratio can also be probed by measuring the $e^-p \rightarrow \nu_e x$ and $e^+p \rightarrow \bar{\nu}_e x$ charged-current DIS, where the underlying processes are $e^-u \rightarrow \nu_e d$ and $e^+d \rightarrow \bar{\nu}_e u$, respectively. The recent H1 charged-current data [25], shown in Fig. 3, indicate that the u quark density at large x ($x = 0.65$) is smaller than expected from the current

PDF parametrization. Very recently, the Fermilab E866/NuSea collaboration reported the absolute Drell-Yan cross sections of 800 GeV $p + p$ and $p + d$ [26]. As shown in Fig. 3, the data fall below the PDF predictions at large x (up to $x = 0.8$). The H1 and the E866 results suggest that u quark density at large x might be smaller than expected from current PDFs. This clearly would impact on the d/u ratio at large x , as shown in a recent global PDF analysis [27].

The uncertainties involved in the extraction of F_2^n from F_2^d data can be greatly reduced using the technique of neutron-tagging. A new experiment [28] has been proposed at the JLab Hall-B to detect $e^- d \rightarrow e^- px$, where a low-energy recoiled proton will be measured in coincidence with the (e, e') scattering. Using this method, the F_2^n/F_2^p ratio over the range $0.2 < x < 0.7$ could be determined with small systematic uncertainties.

TRANSITION FROM HIGH- Q^2 TO LOW- Q^2

Quark-hadron duality

The recent studies at JLab of the spin-averaged and spin-dependent structure functions at low Q^2 region have shed new light on the subject of quark-hadron duality. Thirty years ago, Bloom and Gilman [29] noticed that the structure functions obtained from deep-inelastic scattering experiments, where the substructures of the nucleon are probed, are very similar to the averaged structure functions measured at lower energy, where effects of nucleon resonances dominate. This surprising similarity between the resonance electroproduction and the deep inelastic scattering suggests a common origin for these two phenomena, called local duality.

Recently, high precision data [30] from JLab have verified the quark-hadron duality for spin-averaged scattering on proton and deuteron targets. For Q^2 as low as 0.5 GeV^2 , the resonance data are within 10% of the DIS results. When the mean F_2 curve from the resonance data is plotted as a function of the Nachtmann variable, $\xi = 2x/(1 + \sqrt{1 + 4M^2x^2/Q^2})$, it resembles the xF_3 structure function obtained in neutrino scattering experiments. Since xF_3 is a measure of the valence quark distributions, this suggests that the F_2 structure function at low Q^2 originates from valence quarks only.

The study of quark-hadron duality was recently extended to other structure functions. Results from HERMES [31] show that duality is also observed for the spin-dependent quantity A_1^p . Another recent result from JLab shows that the nuclear modifications to the unpolarized structure functions in the resonance region are in surprisingly good agreement with those measured in DIS [32].

$\Gamma_1(Q^2)$ at low Q^2 and the generalized GDH integral

The extensive data on $g_1(x, Q^2)$ allow accurate determinations of the integrals $\Gamma_1^{p,n}(Q^2) = \int_0^1 g_1^{p,n}(x, Q^2) dx$ for the proton and the neutron, as well as $\Gamma_1^p(Q^2) - \Gamma_1^n(Q^2)$. While the values of Γ_1^p and Γ_1^n are different from the predictions of Ellis and Jaffe who

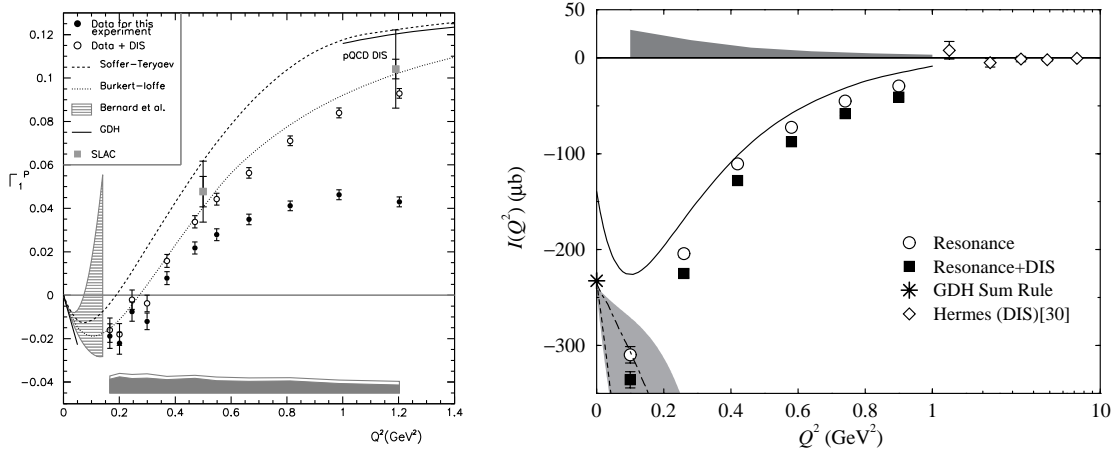


FIGURE 4. Left panel: $\Gamma_1^p(Q^2)$ from CLAS [33]. Right panel: Generalized GDH integral from JLab Hall-A experiment [34].

assumed SU(3) flavor symmetry and an unpolarized strange sea, the data are in good agreement with the prediction of the Bjorken sum rule.

How does $\Gamma_1(Q^2)$ evolve as $Q^2 \rightarrow 0$? This question is closely related to the Gerasimov-Drell-Hearn (GDH) sum rule:

$$\int_{v_0}^{\infty} [\sigma_{1/2}(v) - \sigma_{3/2}(v)] \frac{dv}{v} = -\frac{2\pi^2\alpha}{M^2} \kappa^2. \quad (2)$$

The GDH sum rule, based on general physics principles (causality, unitarity, Lorentz and gauge invariances) and dispersion relation, relates the total absorption cross sections of circularly polarized photons on longitudinally polarized nucleons to the static properties of the nucleons. In Eq. 2, $\sigma_{1/2}$ and $\sigma_{3/2}$ are the photo-nucleon absorption cross sections of total helicity of 1/2 and 3/2, v is the photon energy and v_0 is the pion production threshold, M is the nucleon mass and κ is the nucleon anomalous magnetic moment. The GDH integral in Eq. 2 can be generalized from real photon absorption to virtual photon absorption with non-zero Q^2 :

$$I_{GDH}(Q^2) \equiv \int_{v_0}^{\infty} [\sigma_{1/2}(v, Q^2) - \sigma_{3/2}(v, Q^2)] \frac{dv}{v} = \frac{16\pi^2\alpha}{Q^2} \Gamma_1(Q^2). \quad (3)$$

Eq. 3 shows that the Q^2 -dependence of the generalized GDH integral is directly related to the Q^2 -dependence of Γ_1 . The GDH sum rule (Eq. 2) predicts $\Gamma_1^p = 0$ at $Q^2 = 0$ with a negative slope for $d\Gamma_1^p(Q^2)/dQ^2$ and Γ_1^p is known to be positive at high Q^2 , therefore, $\Gamma_1^p(Q^2)$ must become negative at low Q^2 .

The GDH integrals at low Q^2 have recently been measured in several experiments at JLab [34, 33] and HERMES [35]. Results from a JLab Hall-B measurement [33] of $\Gamma_1^p(Q^2)$ are shown in Fig. 4. These data indeed show that Γ_1^p changes sign around $Q^2 = 0.3 \text{ GeV}^2$. The origin of the sign-change can be attributed to the competition

between $\Delta(1232)$ and higher nucleon resonances. At the lowest Q^2 , the $\Delta(1232)$ has a dominant negative contribution to Γ_1^p . However, at larger Q^2 , higher mass nucleon resonances take over to have a net positive Γ_1^p .

Results [34] from a JLab Hall-A measurement of the generalized GDH integral for neutron using a polarized ^3He target are shown in Fig. 4. In contrast to the proton case, the strong negative contribution to the GDH integral from the $\Delta(1232)$ resonance now dominates the entire measured Q^2 range. Future experiments at JLab will extend the measurements down to $Q^2 = 0.02 \text{ GeV}^2$ in order to map out the low Q^2 behavior of the neutron and proton generalized GDH integrals.

NOVEL DISTRIBUTION AND FRAGMENTATION FUNCTIONS

In addition to the unpolarized and polarized quark distributions, $q(x, Q^2)$ and $\Delta q(x, Q^2)$, a third quark distribution, called transversity, is the remaining twist-2 distribution yet to be measured. This helicity-flip quark distribution, $\delta q(x, Q^2)$, can be described in quark-parton model as the net transverse polarization of quarks in a transversely polarized nucleon. Due to the chiral-odd nature of the transversity distribution, it can not be measured in inclusive DIS experiments. In order to measure $\delta q(x, Q^2)$, an additional chiral-odd object is required. For example, the double spin asymmetry, A_{TT} , for Drell-Yan cross section in transversely polarized pp collision, is sensitive to transversity since $A_{TT} \sim \sum_i e_i^2 \delta q_i(x_1) \delta \bar{q}_i(x_2)$. Such a measurement could be carried out at RHIC [18], although the anticipated effect is small, on the order of 1 – 2%.

Several other methods for measuring transversity have been proposed for semi-inclusive DIS. In particular, Collins suggested [36] that a chiral-odd fragmentation function in conjunction with the chiral-odd transversity distribution would lead to a single-spin azimuthal asymmetry in semi-inclusive pion production.

The HERMES collaboration recently reported [37] observation of single-spin azimuthal asymmetry for charged and neutral hadron electroproduction. Using unpolarized positron beam on a longitudinally polarized hydrogen and deuterium targets, the cross section was found to have a $\sin\phi$ dependence correlating with the target spin direction. ϕ is the azimuthal angle between the pion and the (e, e') scattering plane. This Single-Spin-Asymmetries (SSA) can be expressed as the analyzing power in the $\sin\phi$ moment, and the result is shown in Fig. 5. The $\sin\phi$ moment for an unpolarized (U) positron scattered off a longitudinally (L) polarized target contains two main contributions

$$\langle \sin\phi \rangle \propto S_L \frac{2(2-y)}{Q\sqrt{1-y}} \sum_q e_q^2 x h_L^q(x) H_1^{\perp,q}(z) + S_T (1-y) \sum_q e_q^2 x h_1^q(x) H_1^{\perp,q}(z), \quad (4)$$

where S_L and S_T are the longitudinal and transverse components of the target spin orientation with respect to the virtual photon direction. For the HERMES experiment with a longitudinally polarized target, the transverse component is nonzero with a mean value of $S_T \approx 0.15$. The observed azimuthal asymmetry could be a combined effect of the h_1 transversity and the twist-3 h_L distribution. Recently, another mechanism involving a chiral-even T-odd Sivers distribution function [38] was shown to contribute

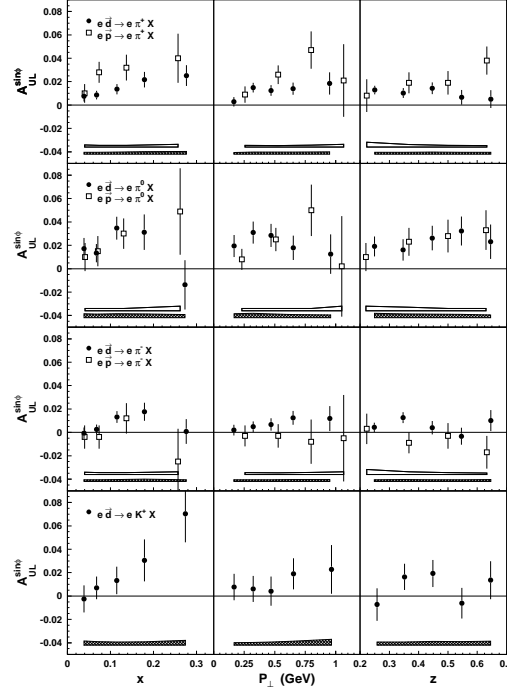


FIGURE 5. Analyzing power in the $\sin\phi$ moment from HERMES [35].

to azimuthal asymmetry [39, 40]. For a longitudinally polarized target the Collins and the Sivers mechanisms can not be distinguished.

If the azimuthal asymmetry observed by HERMES is indeed caused by the h_1 transversity, a much larger asymmetry is expected for a transversely polarized target. The HERMES and COMPASS collaborations have collected polarized SIDIS using transversely polarized hydrogen and ^6LiD targets, respectively. These data would shed much light on the origins of the SSA and could also disentangle the Sivers effect from the Collins effect. The Collins effect has a $\sin(\phi_h^l + \phi_s^l)$ dependence while the Sivers effect is proportional to $\sin(\phi_h^l - \phi_s^l)$, where $\phi_s^l = \phi_s - \phi^l$ is the angle between target spin and the lepton scattering plane. For longitudinally polarized target $\phi_s^l = 0$ and the two effects have identical ϕ dependence. For transversely polarized target, however, $\phi_s^l \neq 0$ and the two effects can be separated.

The Collins fragmentation function represents a correlation between the quark's transverse spin and the transverse momentum of the leading hadron formed in the fragmentation process. The Sivers distribution function reflects the correlation between the quark's transverse spin and its transverse momentum within the proton. It has been shown [41, 42] that both the Collins and the Sivers effects can contribute to the analysing power A_N observed in the Fermilab E704 $p \uparrow p \rightarrow \pi x$ reaction [43]. Very recently, A_N was measured [44] at RHIC at a much higher energy of $\sqrt{s} = 200$ GeV using transversely polarized proton beams. The RHIC data could provide new information on the Collins and Sivers functions.

GENERALIZED PARTON DISTRIBUTIONS

There has been intense theoretical and experimental activities in recent years on the subject of Generalized Parton Distribution (GPD). In the Bjorken scaling regime, exclusive leptonproduction reactions can be factorized into a hard-scattering part calculable in QCD, and a non-perturbative part parameterized by the GPDs. The GPD takes into account dynamical correlations between partons with different momenta. In addition to the dependence on Q^2 and x , the GPD also depends on two more parameters, the skewedness ξ and the momentum transfer to the baryon, t . Of particular interest is the connection between GPD and the nucleon's orbital angular momentum [45].

The deeply virtual Compton scattering (DVCS), in which an energetic photon is produced in the reaction $ep \rightarrow ep\gamma$, is most suitable for studying GPD. Unlike the exclusive meson productions, DVCS avoids the complication associated with mesons in the final state and can be cleanly interpreted in terms of GPDs. An important experimental challenge, however, is to separate the relatively rare DVCS events from the abundant electromagnetic Bethe-Heitler (BH) background. From the collision of 800 GeV protons with 27.5 GeV positrons, both the ZEUS [46] and the H1 [47] collaborations at DESY observed an excess of $e^+ + p \rightarrow e^+ + \gamma + p$ events in a kinematic region where the BH cross section is largely suppressed. The excess events were attributed to the DVCS process and the ZEUS collaboration further determined [46] the DVCS cross section over the kinematic range $5 < Q^2 < 100 \text{ GeV}^2$, $40 < W < 140 \text{ GeV}$. Both the W and Q^2 dependences of the ZEUS DVCS cross section data are well described by calculations based on GPD and on the color-dipole model.

At lower c.m. energies, the HERMES [48] and the CLAS [49] collaborations observed the interference between the DVCS and the BH processes, which manifests itself as a pronounced $\sin\phi$ azimuthal asymmetry correlated with the beam helicity. Another observable sensitive to the interference between the DVCS and the BH processes is the azimuthal asymmetry between unpolarized e^+ and e^- beams. In contrast to the Beam Spin Asymmetry (BSA) which is sensitive to the imaginary part of the DVCS amplitudes, the Beam Charge Asymmetry (BCA) is probing the real part of the DVCS amplitudes [50]. Analysis of the HERMES e^- data in 98-99 and the e^+ data in 99-00 has shown a positive effect for BSA [51].

QCD factorization was proved to be valid for exclusive meson production with longitudinal virtual photons [52]. Such factorization allowed new means to extract the unpolarized and polarized GPD. In particular, unpolarized GPDs can be measured with exclusive vector meson production, while polarized GPDs can be probed via exclusive pseudoscalar meson production. A broad program of DVCS and hard exclusive processes has been proposed [53] for the 12 GeV upgrade at JLab.

ACKNOWLEDGMENTS

I would like to thank V. Burkert, J. P. Chen, C. Keppel, N. Makins, and W. K. Tung for helpful discussion.

REFERENCES

1. Gottfried, K., *Phys. Rev. Lett.*, **18**, 1174 (1967).
2. Towell, R. S., et al., *Phys. Rev.*, **D64**, 052002 (2001).
3. Kumano, S., *Phys. Rep.*, **303**, 183 (1998).
4. Garvey, G. T., and Peng, J. C., *Prog. Part. Nucl. Phys.*, **47**, 203 (2001).
5. Barone, V., et al., *Eur. Phys. J.*, **C12**, 243 (2000).
6. Zeller, G. P., et al., *Phys. Rev.*, **D18**, 111103 (2002).
7. Goncharov, M., et al., *Phys. Rev.*, **D64**, 112006 (2001).
8. Olness, F., *Talk presented at DIS03* (2003).
9. Zeller, G. P., et al., *Phys. Rev. Lett.*, **88**, 091802 (2002).
10. Garvey, G., Louis, W., and White, H., *Phys. Rev.*, **C48**, 761 (1993).
11. Spayde, D. T., et al., *Phys. Rev. Lett.*, **84**, 1106 (2000).
12. Aniol, K. A., et al., *Phys. Lett.*, **B509**, 211 (2001).
13. Diakonov, D. I., et al., *Nucl. Phys.*, **B480**, 341 (1996).
14. Wakamatsu, M., and Kubota, T., *Phys. Rev.*, **D57**, 5755 (1998).
15. Airapetian, A., et al., *hep-ex/0307064* (2003).
16. Dressler, B., et al., *Eur. Phys. J.*, **C14**, 147 (2000).
17. Adeva, B., et al., *Phys. Rev.*, **D58**, 112002 (1998).
18. Bunce, G., et al., *Ann. Rev. Nucl. Part. Sci.*, **50**, 525 (2000).
19. Close, F. E., *Phys. Lett.*, **B43**, 422 (1973).
20. Carlitz, R., *Phys. Lett.*, **B58**, 345 (1975).
21. Farrar, G. R., and Jackson, D. R., *Phys. Rev. Lett.*, **35**, 1416 (1975).
22. Brodsky, S., Burkardt, M., and Schmidt, I., *Nucl. Phys.*, **B441**, 197 (1995).
23. W., M., and Thomas, A. W., *Phys. Lett.*, **B377**, 11 (1996).
24. Abe, F., et al., *Phys. Rev. Lett.*, **81**, 5754 (1998).
25. Zhang, Z., *hep-ph/0110231* (2001).
26. Webb, J. C., et al., *hep-ex/0302019* (2003).
27. Tung, W. K., *Talk presented at DIS03* (2003).
28. Kuhn, S., et al., *JLab proposal E-03-012* (2003).
29. Bloom, E. D., and Gilman, F. J., *Phys. Rev. Lett.*, **25**, 1140 (1970).
30. Niculescu, I., et al., *Phys. Rev. Lett.*, **85**, 1182,1186 (2000).
31. Airapetian, A., et al., *Phys. Rev. Lett.*, **90**, 092002 (2003).
32. Arrington, J., et al., *nucl-ex/0307012* (2003).
33. Fatemi, R., et al., *nucl-ex/0306019* (2003).
34. Amarian, M., et al., *Phys. Rev. Lett.*, **89**, 242301 (2002).
35. Airapetian, A., et al., *hep-ex/0210047* (2002).
36. Collins, J., *Nucl. Phys.*, **B396**, 161 (1993).
37. Airapetian, A., et al., *Phys. Lett.*, **B562**, 182 (2003).
38. Sivers, D. W., *Phys. Rev.*, **D41**, 83 (1990).
39. Brodsky, S., Hwang, D., and Schmidt, I., *Phys. Lett.*, **B530**, 99 (2002).
40. Collins, J., *Phys. Lett.*, **B536**, 43 (2002).
41. Anselmino, M., Boglione, M., and Murgia, F., *Phys. Lett.*, **B362**, 164 (1995).
42. Anselmino, M., and Murgia, F., *Phys. Lett.*, **B442**, 470 (1998).
43. Adams, D. L., et al., *Phys. Lett.*, **B261**, 201 (1991).
44. Bland, L. C., *hep-ex/0212013* (2002).
45. Ji, X., *Phys. Rev. Lett.*, **78**, 610 (1997).
46. Chekanov, S., et al., *hep-ex/0305028* (2003).
47. Adloff, C., et al., *Phys. Lett.*, **B517**, 47 (2001).
48. Airapetian, A., et al., *Phys. Rev. Lett.*, **87**, 182001 (2001).
49. Stepanyan, S., et al., *Phys. Rev. Lett.*, **87**, 182002 (2001).
50. Diehl, M., et al., *Phys. Lett.*, **B411**, 193 (1997).
51. Bianchi, N., *Int. J. Mod. Phys.*, **A18**, 1311 (2003).
52. Collins, J. C., et al., *Phys. Rev.*, **D56**, 2982 (1997).
53. Burkert, V., *hep-ph/0303006* (2003).